MiRNA-488-3p suppresses acute myocardial infarction-induced cardiomyocyte apoptosis *via* targeting ZNF791

H.-F. ZHENG¹, J. SUN², Z.-Y. ZOU³, Y. ZHANG⁴, G.-Y. HOU⁵

Abstract. – OBJECTIVE: The aim of this study was to elucidate the potential function of microRNA-488-3p (miRNA-488-3p) in the pathogenesis of acute myocardial infarction (AMI).

MATERIALS AND METHODS: AMI mice constructed by ligation of the anterior descending coronary artery (LAD) were administrated with miRNA-488-3p mimics or negative control, respectively. Infarct size and risk region of AMI mice were determined by triphenyltetrazolium chloride (TTC) staining. The serum level of lactate dehydrogenase (LDH) release in mice was detected by enzyme-linked immunosorbent assay (ELISA). Subsequently, primary cardiomyocytes were isolated from AMI mice administrated with miRNA-488-3p mimics or negative control. LDH release in both hypoxia-preconditioning primary cardiomyocytes and MCM cells was detected. Dual-Luciferase reporter gene assay was used to verify the potential target of miRNA-488-3p. Furthermore, the regulatory effects of miRNA-488-3p and its target ZNF791 on AMI-induced cardiomyocyte apoptosis were evaluated.

RESULTS: MiRNA-488-3p was lowly expressed in AMI mice. Meanwhile, miRNA-488-3p expression decreased in hypoxia-preconditioning primary cardiomyocytes or MCM cells in a time-dependent manner. AMI mice overexpressing miRNA-488-3p showed significantly smaller infarct size and risk region, as well as lower LHD release in serum. Overexpression of miRNA-488-3p markedly down-regulated the protein level of caspase3 in MCM cells. ZNF791 was predicted as the direct target of miRNA-488-3p, which was negatively regulated by miRNA-488-3p. Overexpression of ZNF791 reversed the protective role of miRNA-488-3p in AMI-induced cardiomyocyte apoptosis.

CONCLUSIONS: MiRNA-488-3p is down-regulated in AMI mice, which alleviates AMI-induced cardiomyocyte apoptosis *via* down-regulating ZNF791.

Key Words: MiRNA-488-3p, ZNF791, AMI.

Introduction

Acute myocardial infarction (AMI) is a critical disease worldwide. The incidence and mortality of AMI have continued to rise in China over the past few decades¹. Vascular occlusion and plaque rupture resulted from coronary atherosclerosis are the leading causes of AMI. Clinically, this is characterized by endothelial damage, lipid accumulation and atherosclerotic plaque formation. Excessive inflammation further leads to cardiomyocyte necrosis and apoptosis, which are the reasons for cardiomyocyte damage and loss². It is known that apoptosis mainly occurs in the ischemic area³. Cardiomyocyte apoptosis triggers cardiac remodeling and pathophysiology of heart failure following AMI. Prevention and reduction of cardiomyocyte apoptosis can improve cardiac dysfunction and cardiac remodeling at post-AMI. This has been confirmed as the key point in AMI treatment⁴. Therefore, it is necessary to uncover the mechanism of AMI-induced cardiomyocyte apoptosis, angiogenesis and myocardial fibrosis, and to search for novel therapeutic targets for AMI.

Micro-ribonucleic acids (miRNAs) are a class of non-coding RNAs with about 20-25 nucleotides in length. They directly bind to the 3'UTR of target mRNAs, further degrading them or inhibiting their translation at post-transcriptional level^{5,6}. MiRNAs have been identified to participate in cardiovascular physiology and pathology.

¹ICU, Chongqing General Hospital, Chongqing, China

²Department of Ultrasound, the Affiliated Hospital of Weifang Medical University, Weifang, China

³Department of Cardiology, The 982th Hospital of Chinese PLA, Tangshan, China

⁴Department of Two Subjects of Convalescence, Naval Qingdao First Sanatorium First Health Care Area, Qingdao, China

⁵Department of Geriatrics, The 89th Hospital of the People's Liberation Army, Weifang, China

Meanwhile, they are involved in the regulation of cardiomyocyte growth and function, including cardiac muscle contraction, electrical conduction, cardiomyocyte phenotypes and neovascularization⁷⁻¹⁰. Recent researches^{3,11-13} have shown that non-coding RNAs, including miRNAs, are involved in pathological events following AMI. Several miRNAs have been proved to exert protective roles in the heart. Previous studies¹⁴⁻²⁰ have indicated that they can protect against apoptosis, hypertrophy, fibroblast activation and inflammatory response. Recently, miRNA-488-3p has been reported differentially expressed in tumor tissues, exerting a vital role in disease progression^{21,22}. However, the biological role of miRNA-488-3p in AMI has not been fully elucidated.

The zinc finger (ZNF) family is one of the largest families in the human genome with 500-600 members^{23,24}. Although the specific functions of most ZNF genes remain unknown, they have been considered to encode transcriptional regulators and participate in cell differentiation. Current studies²⁵ have found that ZNF791 is a representative of the ZNF family.

In this work, we mainly explored the biological role of miRNA-488-3p in AMI and the underlying mechanism. Our findings might provide a novel direction in the clinical treatment of AMI.

Materials and Methods

Establishment of the AMI Model in Mice

C57BL/6 mice with 8-week-old were anesthetized by 1.0-1.5% isoflurane. Subsequently, the mice were connected to the mechanical ventilation device, and a longitudinal incision was made to expose the heart. Muscles and tissues around the heart were then bluntly separated. Ligation of the anterior descending coronary artery (LAD) was performed using 7.0 suture. Meanwhile, mice in the control group were cut open without performing LAD. During LAD procedures, mice were administrated with miRNA-488-3p mimics or negative control, respectively. This study was approved by the Animal Ethics Committee of Chongqing General Hospital Animal Center.

Cell Culture and Transfection

Primary cardiomyocytes and MCM cells were provided by the American Type Culture Collection (ATCC; Manassas, VA, USA). All cells were cultured in Dulbecco's Modified Eagle's Medium/nutrient mixture F-12 (DMEM/F-12; Hyclone, South Logan, UT, USA) containing 15% fetal bovine serum (FBS; Hyclone, South Logan, UT, USA), 1% penicillin-streptomycin and 0.1 mmol/L BrdU (Beyotime, Shanghai, China). After centrifugation at 1000 rpm for 10 min, the cells were re-suspended in the above-mentioned medium for 60 min. Subsequently, the supernatant was collected and transferred to a 65 mm dish. 48 h later, the cells were adherent to the culture dish.

Cell transfection was performed according to the instructions of Lipofectamine 2000 (Invitrogen, Carlsbad, CA, USA). Transfected cells for 48 h were harvested for the following experiments.

Hypoxia Preconditioning

Primary cardiomyocytes and MCM cells in the logarithmic growth phase were subjected to serum starvation for 3 h. Normoxia preconditioning under 20% $\rm O_2$ and 5% $\rm CO_2$, or hypoxia-preconditioning under 2% $\rm O_2$, 5% $\rm CO_2$ and 93% $\rm N_2$ were conducted.

Ouantitative Real Time-Polymerase Chain Reaction (qRT-PCR)

Total RNA was extracted from cells using the TRIzol Reagent (Invitrogen, Carlsbad, CA, USA). Subsequently, extracted RNA was reverse transcribed into complementary deoxyribonucleic acid (cDNA) using the AMV reverse transcription system. SYBR® premixed Dimer EraserTM was used for mRNA expression analysis. Quantitative Real Time-Polymerase Chain Reaction (qRT-PCR) was performed using a StepOne (TM) system (Applied Biosystems, Foster City, CA, USA). QRT-PCR reaction conditions were as follows: 94°C for 30 s, 55°C for 30 s, and 72°C for 90 s, for a total of 40 cycles. The relative expression level of the target gene was calculated by the $2^{-\Delta\Delta Ct}$ method. U6 was used as an internal reference in quantitative analysis of miRNA-488-3p expression. Glyceraldehyde 3-phosphate dehydrogenase (GAPDH) was used as an internal reference in quantitative analysis of large tumor suppressor kinase 2 expression. The experiment was repeated 3 times. Primer sequences used in this study were as follows: ZNF791, F: 5'-CGCCTAGGGCCCCGCGTTGCTC-3', R: 5'-GCTAGTGATGGTGGACAGGA-3'; miRNA-488-3p, F: 5'-GATGCCCACATGCTCGACATG-3', R: 5'-GGATTGATGTTTGGAGGCG-3'; U6: F: 5'-GCTTCGGCAGCACATATACTAAAAT-3', R: 5'-CGCTTCAGAATTTGCGTGTCAT-3'; GAP-DH: F: 5'-CGCTCTCTGCTCCTGTTC-3', R: 5'-ATCCGTTGACTCCGACCTTCAC-3'.

Dual-Luciferase Reporter Gene Assay

The transcript 3'untranslated region (3'UTR) sequence of ZNF791 was first cloned into vector pGL3 containing Luciferase reporter gene, namely ZNF791 WT. ZNF791 MUT was constructed by mutating the core binding sequences using a site-directed mutagenesis kit (Thermo Fisher Scientific, Waltham, MA, USA). Subsequently, the cells were co-transfected with miRNA-488-3p mimic/negative control and ZNF791 WT/MUT. At 48 h, the cells were lysed for determining Luciferase activity.

Western Blot

Total protein in cells or tissues was extracted using radio-immunoprecipitation assay (RIPA; Beyotime, Shanghai, China). The concentration of extracted protein was determined by the bicinchoninic acid (BCA) method. Protein samples were electrophoresed on polyacrylamide gels and transferred onto polyvinylidene difluoride (PVDF) membranes (Millipore, Billerica, MA, USA). After blocking with 5% skimmed milk, the membranes were incubated with primary antibodies (Abcam, Cambridge, MA, USA) at 4°C overnight. After rinsing with Tris-Buffered Saline and Tween 20 solution (TBST; Sigma-Aldrich, St. Louis, MO, USA), the membranes were incubated with corresponding secondary antibody (Abcam, Cambridge, MA, USA). Immunoreactive bands were exposed by enhanced chemiluminescence (ECL: Thermo Fisher Scientific, Waltham, MA, USA) and analyzed by Image Software (NIH, Bethesda, MD, USA).

Determination of Lactate Dehydrogenase (LDH) Release

The supernatant of cultured cells was collected for determination of LDH level. LDH release was measured in strict accordance with the CytoTox 96 non-radioactive cytotoxicity assay kit (Sigma-Aldrich, St. Louis, MO, USA). The serum level of LDH was determined by enzyme-linked immunosorbent assay (ELISA; Novus Biologicals, Littleton, CO, USA).

Determination of Infarct Size

Mouse heart was sliced into 2-mm sections, weighed and incubated with triphenyltetrazolium chloride (TTC; Solarbio, Beijing, China) for 15 min in the dark. After washing with Phosphate-Buffered Saline (PBS; Gibco, Grand Island, NY, USA) three times, the sections were fixed with 4% paraformaldehyde and captured

under a microscope (Nikon, Tokyo, Japan). Risk region (including the infarct zone and infarct border zone) was not stained blue by Evans Blue (Sigma-Aldrich, St. Louis, MO, USA), whereas infarct border zone was stained red with TTC. Infarct area was pale. Infarct size = (AMI area per section/section area \times section weight) Σ /left ventricular weight \times 100%.

Statistical Analysis

Statistical Product and Service Solutions (SPSS) 20.0 (SPSS, Chicago, IL, USA) and GraphPad (Version X; La Jolla, CA, USA) were used for all statistical analysis. Experimental data were represented as mean \pm standard deviation (SD). The *t*-test was used to compare the differences between the two groups. One-way analysis of Variance (ANOVA) was applied to compare the differences among different groups, followed by the Post-hoc test. p<0.05 was considered statistically significant.

Results

MiRNA-488-3p Was Down-Regulated at Post-AMI

24 h after LAD, infarct size and risk region in AMI mice were determined by TTC staining. Significantly higher infarct size/risk region and risk region/left ventricle were observed in AMI mice relative to controls (Figure 1A, 1B). The serum level of LDH was markedly higher in AMI mice, suggesting the successful construction of the AMI model in mice (Figure 1C). QRT-PCR data revealed that miRNA-488-3p level decreased at post-AMI in a time-dependent manner (Figure 1D). Hypoxia is the leading factor for cardiomyocyte apoptosis following AMI. Subsequently, primary cardiomyocytes extracted from AMI mice and MCM cells were subjected to hypoxia conditioning. At 3, 6 and 12 h, LDH release decreased gradually in hypoxia-preconditioning primary cardiomyocytes and MCM cells (Figure 1E, 1F).

ZNF791 Was the Target Gene of MiRNA-488-3p

Binding sequences between miRNA-488-3p and ZNF791 were predicted by TargetScan (www.targetscan.org). The results showed that ZNF791 was the candidate target gene of miRNA-488-3p (Figure 2A). Transfection of miRNA-488-3p mimics significantly up-regulated the mRNA level of ZNF791 in MCM cells (Figure 2B).

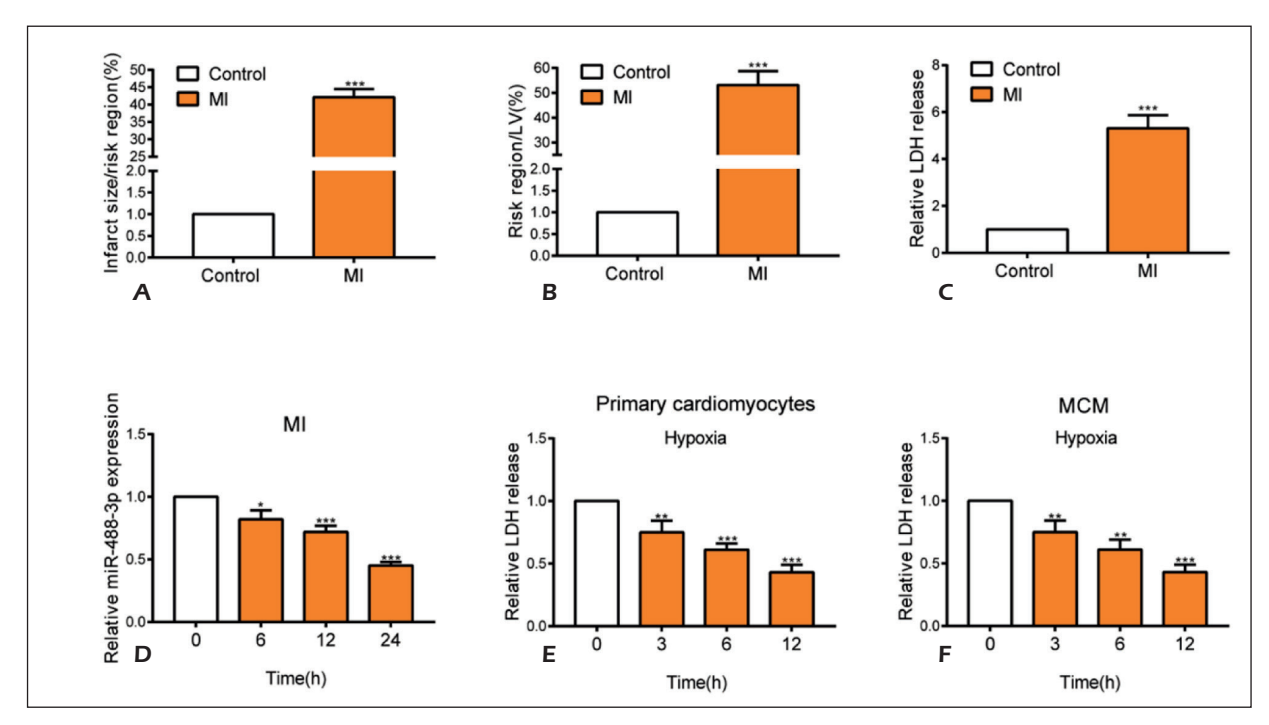


Figure 1. MiR-488-3p was down-regulated at post-AMI. **A**, Infarct size/risk region in AMI and control mice determined by TTC staining at 24 h after LAD. **B**, Risk region/left ventricle in AMI and control mice determined by TTC staining at 24 h after LAD. **C**, Serum level of LDH in AMI and control mice at 24 h after LAD. **D**, Relative level of miR-488-3p at 0, 6, 12 and 24 h following AMI. E, Serum level of LDH at 0, 3, 6 and 12 h in hypoxia-preconditioning primary cardiomyocytes extracted from AMI mice. F, Serum level of LDH at 0, 3, 6 and 12 h in hypoxia-preconditioning MCM cells.

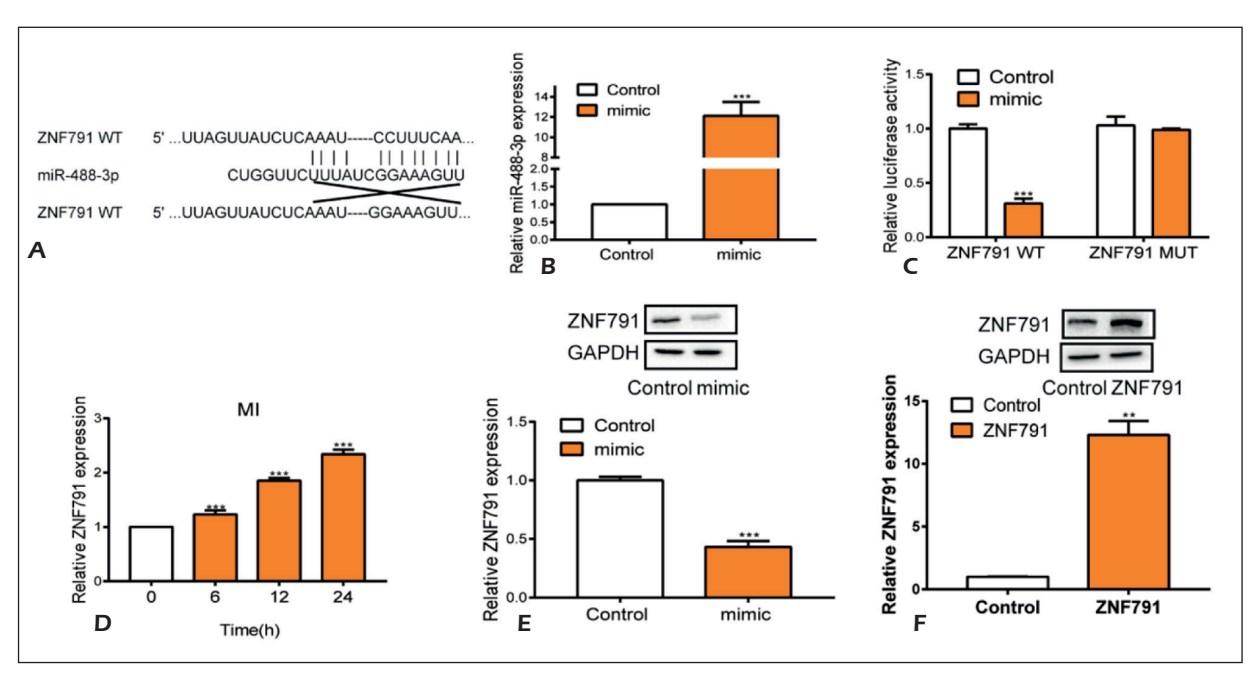


Figure 2. ZNF791 was the target gene of miR-488-3p. **A**, Binding sequences between miR-488-3p and ZNF791 predicted by TargetScan. **B**, Transfection efficacy of miR-488-3p mimics in MCM cells was verified. **C**, Luciferase activity in MCM cells co-transfected with miR-488-3p mimic/negative control and ZNF791 WT/MUT. **D**, Relative level of ZNF791 at 0, 6, 12 and 24 h following AMI. **E**, Protein and mRNA levels of ZNF791 in MCM cells transfected with miR-488-3p mimic or negative control. F, Transfection efficacy of ZNF791 overexpression plasmid in MCM cells was verified.

Furthermore, Luciferase activity decreased significantly in MCM cells co-transfected with miRNA-488-3p mimics and ZNF791 WT. This verified the binding relationship between miRNA-488-3p and ZNF791 (Figure 2C). Within the first 24 h following AMI, ZNF791 level increased gradually in AMI mice (Figure 2D). Both the mRNA and protein levels of ZNF791 were remarkably down-regulated after overexpression of miRNA-488-3p in MCM cells (Figure 2E). To further reveal the potential function of ZNF791 at post-AMI, ZNF791 overexpression plasmid was constructed and its transfection efficacy was verified (Figure 2F).

MiRNA-488-3p Suppressed AMI-Induced Cardiomyocyte Apoptosis

Western blotting showed that the protein level of caspase3 was markedly up-regulated by hypoxia conditioning in MCM cells relative to those with normoxia treatment (Figure 3A). After transfection of ZNF791 overexpression plasmid in hypoxia-preconditioning MCM cells, the

level of caspase3 was significantly up-regulated (Figure 3B). Conversely, overexpression of miR-NA-488-3p in hypoxia-preconditioning MCM cells down-regulated caspase3 expression (Figure 3C). To elucidate the function of miRNA-488-3p *in vivo*, AMI mice were administrated with miRNA-488-3p mimic or negative control, respectively. AMI mice overexpressing miRNA-488-3p presented remarkably lower infarct size/risk region, risk region/left ventricle and serum level of LDH (Figure 3D-3F). The above results suggested that miRNA-488-3p overexpression alleviated AMI-induced cardiomyocyte apoptosis and reduced infarct size.

MiRNA-488-3p Suppressed AMI-Induced Cardiomyocyte Apoptosis Via ZNF791

A series of rescue experiments were conducted to elucidate the role of miRNA-488-3p/ZNF791 following AMI. Down-regulation of caspase3 due to miRNA-488-3p overexpression in MCM cells was reversed by overexpression of ZNF791 (Fig-

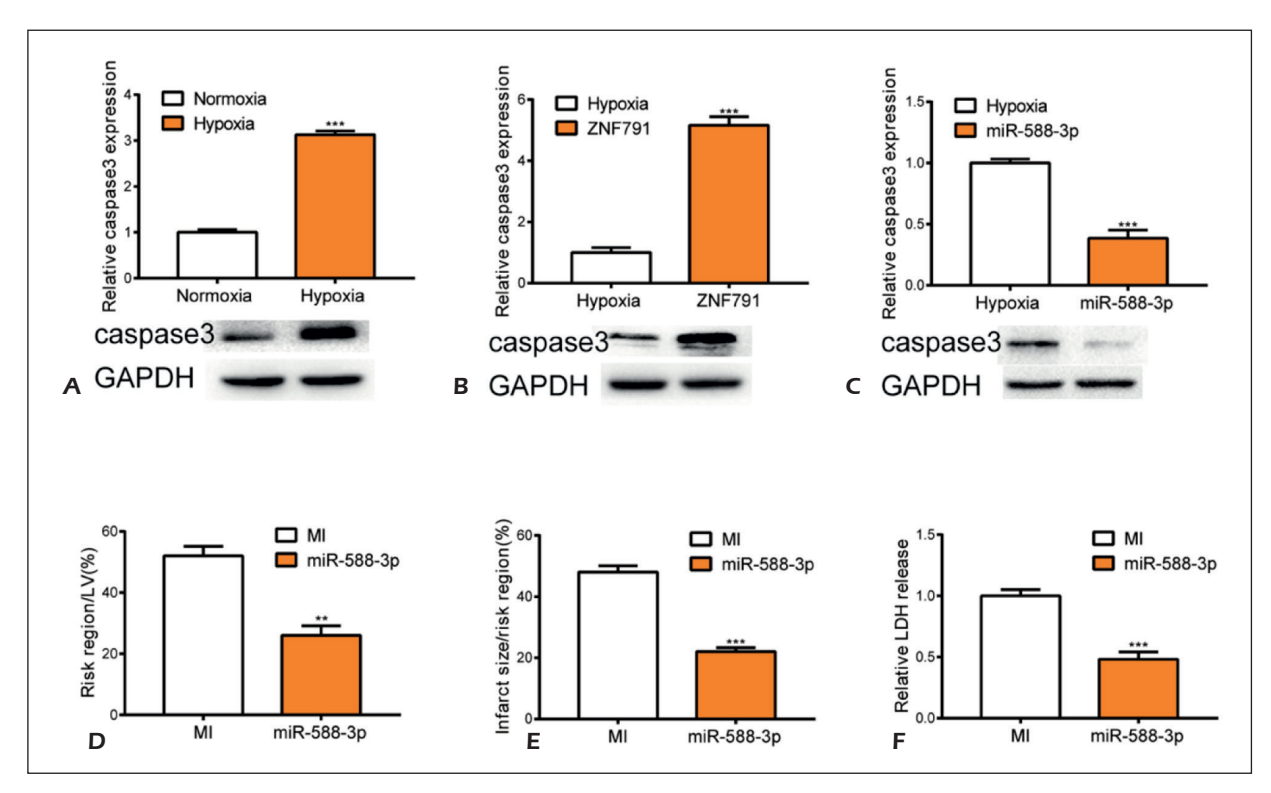


Figure 3. MiR-488-3p suppressed AMI-induced cardiomyocyte apoptosis. **A**, Relative level of caspase3 in hypoxia-preconditioning or normoxia-preconditioning MCM cells. **B**, Relative level of caspase3 in hypoxia-preconditioning MCM cells transfected with ZNF791 overexpression plasmid or negative control. **C**, Relative level of caspase3 in hypoxia-preconditioning MCM cells transfected with miR-488-3p mimic or negative control. **D**, Risk region/left ventricle in AMI mice administrated with miR-488-3p mimic or negative control. **E**, Infarct size/risk region in AMI mice administrated with miR-488-3p mimic or negative control. **E**, Serum level of LDH in AMI mice administrated with miR-488-3p mimic or negative control.

ure 4A). Similarly, the protective effects of miR-NA-488-3p on reducing infarct size/risk region, risk region/left ventricle and serum level of LDH were partially reversed by ZNF791 overexpression (Figure 4B-D). The above findings illustrated that miRNA-488-3p protected cardiomyocytes from AMI damage *via* targeting ZNF791.

Discussion

Apoptosis is important programming for regulating cell death. It is active cell death programmed and regulated by some genes, also known as programmed death²⁷. Reduction of cardiomyocyte apoptosis in infarct area contributes to improving cell survival and adverse events of AMI. In this study, we first established the AMI model in mice. The role of miRNA-488-3p at post-AMI was explored as well. Furthermore, we predicted and analyzed the target gene downstream of miRNA-488-3p in the performances of AMI.

MiRNA-488-3p has been found to act as a tumor suppressor in prostate cancer and gastric cancer^{28,29}. However, its role in AMI has not been fully elucidated. In this work, miRNA-488-3p expression was significantly down-regulated in AMI mice, which decreased in hypoxia-preconditioning primary cardiomyocytes and MCM

cells in a time-dependent manner. Several miR-NAs have been found dysregulated following AMI³⁰. They may suppress cell apoptosis and reduce tissue damage, therefore alleviating pathological lesions following AMI. Current studies³¹ have reported that overexpression of miR-210 in AMI mice suppresses cardiomyocyte apoptosis through down-regulating PP2C β to activate the PI3K/AKT pathway. MiR-182 has been confirmed down-regulated in the ischemia-reperfusion rat model. Meanwhile, it inhibits cardiomyocyte apoptosis by down-regulating BNIP332. In this work, overexpression of miRNA-488-3p remarkably decreased infarct size/risk region, risk region/left ventricle and LDH release in AMI mice. Overexpression of miRNA-488-3p markedly decreased caspase3 expression, suggesting that miRNA-488-3p could suppress AMI-induced apoptosis.

The underlying mechanism of miRNA is mainly related to its target genes³³. MiRNA can negatively mediate gene expression by directly binding to the 3'UTR of target genes, thereby inducing mRNA dysregulation and translational inhibition³⁴. In this study, we predicted the downstream gene of miRNA-488-3p using TargetScan. The results predicted that ZNF791 was a potential target gene for miRNA-488-3p. Their binding relationship was confirmed by Dual-Luciferase re-

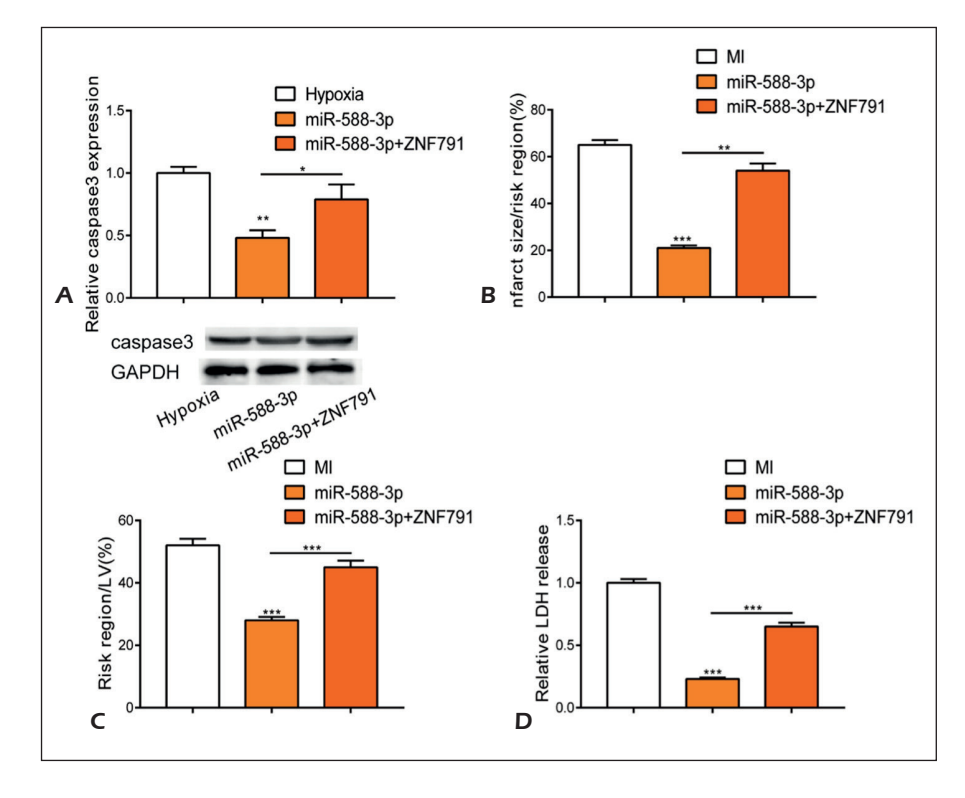


Figure 4. MiR-488-3p suppressed AMI-induced diomyocyte apoptosis via ZNF791. Hypoxia-preconditioning MCM cells were transfected with negative control, miR-488-3p mimic or miR-488-3p mimic+ZNF791 overexpression plasmid, respectively. A, Relative level of caspase3. B, Infarct size/ risk region. C, Risk region/left ventricle and D, Serum level of LDH.

porter gene assay. In addition, ZNF791 was found significantly up-regulated in AMI, and its level was negatively regulated by miRNA-488-3p. In hypoxia-preconditioning cells, ZNF791 overexpression up-regulated caspase3 level. A series of rescue experiments were conducted to elucidate the role of miRNA-488-3p/ZNF791 in AMI. Notably, ZNF791 overexpression partially reversed the protective role of miRNA-488-3p in AMI.

Conclusions

We found that miRNA-488-3p is down-regulated in AMI mice, which alleviates AMI-induced cardiomyocyte apoptosis *via* down-regulating ZNF791.

Conflict of Interests

The authors declare that they have no conflict of interest.

References

- ZHOU M, ZOU YG, XUE YZ, WANG XH, GAO H, DONG HW, ZHANG Q. Long non-coding RNA H19 protects acute myocardial infarction through activating autophagy in mice. Eur Rev Med Pharmacol Sci 2018; 22: 5647-5651.
- OROGO AM, GUSTAFSSON AB. Cell death in the myocardium: my heart won't go on. IUBMB Life 2013; 65: 651-656.
- Guo Y, Luo F, Liu Q, Xu D. Regulatory non-coding RNAs in acute myocardial infarction. J Cell Mol Med 2017; 21: 1013-1023.
- FIEDLER J, THUM T. MicroRNAs in myocardial infarction. Arterioscler Thromb Vasc Biol 2013; 33: 201-205.
- 5) Rios JM. [The big world of the small RNAs]. Rev Latinoam Microbiol 2006; 48: 73-78.
- 6) Wagner S, Willenbrock S, Nolte I, Murua Escobar H. Comparison of non-coding RNAs in human and canine cancer. Front Genet 2013; 4: 46.
- Verjans R, van Bilsen M, Schroen B. MiRNA deregulation in cardiac aging and associated disorders. Int Rev Cell Mol Biol 2017; 334: 207-263.
- 8) Boon RA, Iekushi K, Lechner S, Seeger T, Fischer A, Heydt S, Kaluza D, Treguer K, Carmona G, Bonauer A, Horrevoets AJ, Didier N, Girmatsion Z, Biliczki P, Ehrlich JR, Katus HA, Muller OJ, Potente M, Zeiher AM, Hermeking H, Dimmeler S. MicroRNA-34a regulates cardiac ageing and function. Nature 2013; 495: 107-110.
- WAHLOUIST C, JEONG D, ROJAS-MUNOZ A, KHO C, LEE A, MITSUYAMA S, VAN MIL A, PARK WJ, SLUIJTER JP, DOEVENDANS PA, HAJJAR RJ, MERCOLA M. Inhibition of miR-25 improves cardiac contractility in the failing heart. Nature 2014; 508: 531-535.

- 10) Bonauer A, Carmona G, Iwasaki M, Mione M, Koyanagi M, Fischer A, Burchfield J, Fox H, Doe-Bele C, Ohtani K, Chavakis E, Potente M, Tjwa M, Urbich C, Zeiher AM, Dimmeler S. MicroRNA-92a controls angiogenesis and functional recovery of ischemic tissues in mice. Science 2009; 324: 1710-1713.
- 11) Sun T, Dong YH, Du W, Shi CY, Wang K, Tario MA, Wang JX, Li PF. The role of microRNAs in myocardial infarction: from molecular mechanism to clinical application. Int J Mol Sci 2017; 18: 223.
- 12) FIEDLER J, JAZBUTYTE V, KIRCHMAIER BC, GUPTA SK, LO-RENZEN J, HARTMANN D, GALUPPO P, KNEITZ S, PENA JT, SOHN-LEE C, LOYER X, SOUTSCHEK J, BRAND T, TUSCHL T, HEINEKE J, MARTIN U, SCHULTE-MERKER S, ERTL G, ENGELHARDT S, BAUERSACHS J, THUM T. MICTORNA-24 regulates vascularity after myocardial infarction. Circulation 2011; 124: 720-730.
- 13) HINKEL R, PENZKOFER D, ZÜHLKE S, FISCHER A, HUSA-DA W, XU Q, BALOCH E, VAN ROOIJ E, ZEIHER AM, KUPATT C, DIMMELER S. Inhibition of microRNA-92a protects against ischemia/reperfusion injury in a large-animal model. Circulation 2013; 128: 1066-1075.
- 14) ONG SG, LEE WH, HUANG M, DEY D, KODO K, SANCHEZ-FREIRE V, GOLD JD, Wu JC. Cross talk of combined gene and cell therapy in ischemic heart disease: role of exosomal microRNA transfer. Circulation 2014; 130: S60-S69.
- 15) Hosoda T, Zheng H, Cabral-da-Silva M, Sanada F, Ide-Iwata N, Ogorek B, Ferreira-Martins J, Arranto C, D'Amario D, Del MF, Urbanek K, D'Alessandro DA, Michler RE, Anversa P, Rota M, Kajstura J, Leri A. Human cardiac stem cell differentiation is regulated by a mircrine mechanism. Circulation 2011; 123: 1287-1296.
- 16) PAN Z, SUN X, SHAN H, WANG N, WANG J, REN J, FENG S, XIE L, Lu C, YUAN Y, ZHANG Y, WANG Y, Lu Y, YANG B. MicroRNA-101 inhibited postinfarct cardiac fibrosis and improved left ventricular compliance via the FBJ osteosarcoma oncogene/transforming growth factor-beta1 pathway. Circulation 2012; 126: 840-850.
- 17) Hu S, Huang M, Li Z, Jia F, Ghosh Z, Lijkwan MA, Fasanaro P, Sun N, Wang X, Martelli F, Robbins RC, Wu JC. MicroRNA-210 as a novel therapy for treatment of ischemic heart disease. Circulation 2010; 122: S124-S131.
- 18) Dong S, Cheng Y, Yang J, Li J, Liu X, Wang X, Wang D, Krall TJ, Delphin ES, Zhang C. MicroRNA expression signature and the role of microRNA-21 in the early phase of acute myocardial infarction. J Biol Chem 2009; 284: 29514-29525.
- 19) TIAN Y, LIU Y, WANG T, ZHOU N, KONG J, CHEN L, SNITOW M, MORLEY M, LI D, PETRENKO N, ZHOU S, LU M, GAO E, KOCH WJ, STEWART KM, MORRISEY EE. A microRNA-Hippo pathway that promotes cardiomyocyte proliferation and cardiac regeneration in mice. Sci Transl Med 2015; 7: 238r-279r.
- 20) ZHOU X, SUN F, LUO S, ZHAO W, YANG T, ZHANG G, GAO M, LU R, SHU Y, MU W, ZHUANG Y, DING F, XU C, LU Y. Let-7a is an antihypertrophic regulator in the heart via targeting calmodulin. Int J Biol Sci 2017; 13: 22-31.

- 21) MUINOS-GIMENO M, ESPINOSA-PARRILLA Y, GUIDI M, KA-GERBAUER B, SIPILA T, MARON E, PETTAI K, KANANEN L, NAVINES R, MARTIN-SANTOS R, GRATACOS M, METSPALU A, HOVATTA I, ESTIVILL X. Human microRNAs miR-22, miR-138-2, miR-148a, and miR-488 are associated with panic disorder and regulate several anxiety candidate genes and related pathways. Biol Psychiatry 2011; 69: 526-533.
- 22) Song J, Kim D, Lee CH, Lee MS, Chun CH, Jin EJ. MicroRNA-488 regulates zinc transporter SLC39A8/ZIP8 during pathogenesis of osteoarthritis. J Biomed Sci 2013; 20: 31.
- 23) HOOVERS JM, MANNENS M, JOHN R, BLIEK J, VAN HEYNINGEN V, PORTEOUS DJ, LESCHOT NJ, WESTERVELD A, LITTLE PF. High-resolution localization of 69 potential human zinc finger protein genes: a number are clustered. Genomics 1992; 12: 254-263.
- 24) BECKER KG, NAGLE JW, CANNING RD, BIDDISON WE, OZATO K, DREW PD. Rapid isolation and characterization of 118 novel C2H2-type zinc finger cDNAs expressed in human brain. Hum Mol Genet 1995; 4: 685-691.
- 25) PIELER T, BELLEFROID E. Perspectives on zinc finger protein function and evolution--an update. Mol Biol Rep 1994; 20: 1-8.